VIII International Conference on Computational Methods for Coupled Problems in Science and Engineering
COUPLED PROBLEMS 2019
E. Oñate, M. Papadrakakis and B. Schrefler (Eds)

FRAMEWORK FOR FLUID-STRUCTURE INTERACTION SIMULATIONS WITH UZEN AND PRECICE: SIMULATIONS PROCEDURE AND VALIDATION

Davide Cinquegrana*, **Pier Luigi Vitagliano**†

* Italian Aerospace Research Centre (CIRA)
Department of Fluid Mechanics, Computational Fluid Dynamics Lab.
Via Maiorisi, 80143, Capua, Italy
e-mail: d.cinquegrana@cira.it, web page: http://www.cira.it/

†Italian Aerospace Research Centre (CIRA)
Department of Fluid Mechanics, Computational Fluid Dynamics Lab.
Via Maiorisi, 80143, Capua, Italy
e-mail: p.vitagliano@cira.it, web page: http://www.cira.it

Key words: FSI, load transfer, time coupling, panel flutter

Abstract.

The paper illustrates a new framework developed to face with Fluid Structure Interaction phenomena in a partitioned approach. The CIRA multi-block structured flow solver[1] for unsteady RANS equations, UZEN, was updated and tightly coupled with an open-source FEM code CalculiX[2]. The solvers are glued in space and time through an open source library, preCICE[3] to deliver exchanging data. preCICE manages the communications, loads mapping and time coupling.

Motivation of the work is the simulation of unsteady aerodynamic problems strongly dependent upon structural behaviour, like flexible aircraft, rotor-craft, counter-rotating rotors, etc.

As validation tests, the results of 2D and 3D panel flutter response at supersonic velocity are illustrated. The results are compared in terms of Limit Cycle Oscillation amplitude and frequency of panel flutter with data available in literature.

1 INTRODUCTION

In the present work, a multi-block structured flow solver[4] for unsteady RANS equations has been coupled with a structural solver within the software environment managed by the open source library preCICE [3], in order to perform fluid-structure interaction simulations.

preCICE (Precise Code Interaction Coupling Environment) is a coupling library for partitioned multi-physics simulations. The software offers methods for transient equation coupling, communication means, and data mapping schemes.

An adapter that delivers exchanging data from CFD solver to preCICE library has been developed, that translates data from CFD to the interfaces, and receives data from FEM solver through preCICE. The loads transfer, or space coupling, is afforded within the library with different techniques, such as Nearest-Neighbour or RBF; the time coupling and convergence check are also managed by the schemes available in the library.

Motivation of the work is the simulation of unsteady aerodynamic problems strongly dependent from structural behaviour, like flexible aircraft, rotor-craft, counter-rotating rotors, or in the framework of airplane weight minimization, where flow induced vibrations influence stability and durability of aircraft[5, 6].

Structural solver, already interfaced within the preCICE framework, is the open source FEM code Calculix[7].

The choice of the preCICE framework was driven by several reasons: the open source environment (no costs and limitations stemming from licences), possibility of testing both explicit and implicit fluid-structure interaction, several interpolation and exchange methods for forces and deformations already available and implemented. Finally the library has been developed with the aim of allowing efficient usage of massively parallel computing architectures[8]. At the same time, the FEM solver, Calculix, is already coupled with an official adapter. The package is able to perform linear and non-linear analysis of static and dynamic problems.

As far as we know, this is the only CFD system based upon structured multi-block meshes fully integrated with a structural dynamic solver for unsteady simulations with dynamic meshes.

To validate the FSI framework, 2D and 3D inviscid panel flutter at supersonic speed is investigated. The problem of instability of plates in gas flow has been studied and reported in literature. In supersonic flow, the instability has the oscillatory nature known as flutter, that can be distinguished in coupled or single-mode flutter[9]. Several time-domain simulations of non-linear panel flutter were performed from transonic to supersonic flows by several authors [10, 11, 9, 12, 13]. From their results at supersonic Mach number flows we should expect high frequency Limit Cycle Oscillations (LCO).

Since it was discovered, inter alia in the 60s at NASA on the Atlas-Centaur and Saturn V rocket, considerable effort was spent to investigate the impact on panel flutter of several structural and aerodynamic parameters. Due to the great cost and complexity involved in supersonic wind tunnel tests, panel flutter has always been studied mainly via mathematical and numerical modelling. Focusing on the aerodynamics side of numerical approach (i.e. the kind of solvers coupled to structural ones to model the aeroelastic phenomena), in the decade going from 50s to 70s theoretical studies have considered different aerodynamic modelling: from the linear piston-theory, a quasi-steady relation between pressure and panel deflection valid for high supersonic Mach numbers in Von Karman's plate the-

ory to the unsteady linearized potential flow theory, and to the unsteady 'shear flow' theory developed by Dowell[14] that takes in account the viscous effects in the boundary layer on the aeroelastic behavior.

Recent works have introduced FEM and CFD solvers to investigate panel flutter in high subsonic and low supersonic flows. Euler equations and FEM were coupled to study non-linear Karman plate equations [10], Navier-Stokes equations to take in account the unsteady viscous laminar boundary layer were introduced in flutter studies by Gordinier and Visbal [11] for the solution of non-linear Karman plate equations again. Hashimoto [12] involved RANS computations to take in account the effects of a turbulent boundary layer, confirming that the boundary layer has a stabilizing effect on the flutter. Also Alder [15] focused on the effects of the turbulent boundary layer defining the stability limits and post flutter characteristics of a 2D and 3D simply supported panel.

Recently, Hejranfar[16] employed a second-order central-difference cell-vertex finite volume method to study 2D panel flutter in inviscid compressible flow: unsteady Euler equations governing fluid flows in the arbitrary Lagrangian-Eulerian form and the large deformation of the solid structure is considered to be governed by the Cauchy equations formulated in the total Lagrangian form. In his study, on the FEM solver side, the panel is modelled with plane strain element, where also the thickness is modelled in order to compute the stress distribution.

In this paper the results of two and three-dimensional analyses of panel flutter are shown, after presenting the two solvers and the way they are coupled by means of preCICE library. The 2D panel flutter analysis is suited to set up the numerical approaches to face with the problem, verifying time and space convergence of the solutions. Finally, the results of the flutter of square and rectangular 3D plates are compared with literature data.

2 Aerodynamic Solver

ZEN is a multi-block structured flow solver developed at CIRA for the U-RANS equations with classical ALE formulation[17, 1]. The spatial discretization is based upon cell-centred finite volumes discretization, with second and fourth order artificial dissipation. The unsteady computations are carried out by using an implicit second order backward difference method together with dual time stepping toward steady state for each physical time step.

CIRA has recently developed a system for flow simulation[4] which allows the non-conformal block to block coupling (i.e. sliding mesh) and dynamic mesh on block base (i.e. some specific blocks in the flow field can be deformed and updated at each time step). Mesh is updated outside the flow solver, which makes possible to iterate with other systems to compute, in a segregated approach, structural deformation, body dynamics and possibly other physical phenomena. Dynamic meshes are implemented by following the 3 step backward implicit time scheme in such a way to satisfy the discrete geometrical conservation law (DGCL[6]). The updated mesh is reloaded at each time step, which

allows to post-process surface deformations due to structural dynamics and, possibly, body dynamics outside the flow solver. It is possible to apply dynamic mesh modifications only in some blocks, to save computational time. The code is adapted to face with FSI problem: in detail, to allows a strong-coupling, the current time step calculations can be repeated (and the updated mesh reloaded), when required, under control of external routines that check for suitable convergence criteria. This will described in details in the following sections.

The flow simulation system communicates by delivering local forces on specific mesh surfaces, as specified in a set-up file, and it is capable to re-mesh the flow domain starting from a set of updated geometric entities like surfaces, curves and vertices, by following specific directives. Geometric entities can be specified or modified by control points.

The adapter code developed for ZEN code is designed as a stand alone software that synchronizes communications with preCICE library, sending and receiving data to and from interface grids. It will be described in the following sections.

3 Structural Solver

CalculiX is a free/open-source (GPL) Finite Element package, developed at the MTU Aero Engines, currently coupled with preCICE with an official adapter in order to face with Fluid-Structure Interaction (structure part), Conjugate Heat Transfer (solid part). Through its adapter CalculiX can write displacement, temperature, heat flux, sink temperature, heat transfer coefficient and can read force, temperature, heat Flux, sink Temperature, heat transfer coefficient. According to the type of analysis, different solvers are available: linear and non-linear, implicit and explicit solver (CCX), written by Guido Dhondt[7, 2]. Those solvers are implemented in C and Fortran modules.

The implicit solver uses incomplete Cholesky pre-conditioning and the iterative solver by Rank and Ruecker [7], which is based on the algorithms by Schwarz [2]. The equation of motion is integrated in time using the α-method developed by Hilber, Hughes and Taylor[7]. This implicit scheme is unconditionally stable and second-order accurate when the α parameter lies in the interval [-1/3,0], in order to controls the high frequency dissipation: α=0 corresponds to the classical Newmark method inducing no dissipation at all, while α=-1/3 corresponds to maximum dissipation[2].

In this work, Calculix is employed to carry out non-linear analysis of structural dynamic problems. A ready-to use adapter able to communicate through preCICE is already available[18].

4 FLUID - STRUCTURE COUPLING: preCICE

This section describes the way CFD and FEM solvers are coupled in a partitioned approach. The aim is to achieve convergence towards solution in every time step by executing each solver independently.

In the context of a partitioned approach, crucial aspects are the load and deformations

transfer over the interfaces shared by the different computational domains, and the time coupling of the different solutions, in order to ensure convergence at each time iteration. Momentum and energy exchanged between the two sub-systems have to be conserved, otherwise the spurious work introduced leads to instabilities divergence of the solution. The introduction or removal of spurious energy by the interface scheme may affect the overall stability properties of the aeroelastic system [19]. Hence, the time synchronization and the transfer of information at interface for non-matching space discretization influence the stability of the algorithm.

The coupling between the two solvers is managed by the open-source preCICE library. The library treats the numerical methods for equation's coupling among the different solvers involved in the multi-physics simulations.

From the structural solver side, the architecture illustrated by Rush[3] is adopted, i.e. the Calculix solver has its adapter that exchanges data with CFD solver through preCICE library. From the CFD solver side, a black-box adapter coupled with a bash script that is able to manage the timing processes and the ZEN-interface with preCICE was developed.

The adapter interface developed in this framework is designed as a stand-alone code, not fully integrated within the CFD solver. Only the communication toward the FEM direction is managed by preCICE: this is configured with a point-to-point based on TCP/IP socket. The communications between CFD and preCICE direction, are based on file-transfer.

4.1 Time-coupling

A coupling scheme describes the logical execution order of two participants In the partitioned approach it is possible to distinguish between a weakly (explicit) and fully coupled (implicit) schemes: the former solves the fluid and solid sub-domains in a staggered fashion without convergence or residual checks, and the stability of this procedure is dependent on density ratio (structure vs fluid), temporal discretization precision order, fluid velocity and flow compressibility[20]. The latter approach foresees that both solvers are executed multiple times until convergence criteria are satisfied at the end of each time step. To this family belong the Block Gauss-Seidel (BGS), the Newton and quasi-Newton strategies.

In the preCICE library either explicit and implicit coupling schemes are available, with the possibility to apply different convergence criteria.

Furthermore, either serial or parallel executions can be selected. Serial refers to the staggered execution of one participant after the other. Parallel refers to the simultaneous execution of both participants.

The strong coupling approaches transform the coupling conditions into Fixed Point Formulation or Equation (FPE). The kind of FPE used determines the execution sequence of the two solvers. One is the staggered execution (see Figure 1), while two parallel approaches introduced by preCICE developers are showed in figure 2, both allowing for the simultaneous execution of fluid and structure solver.

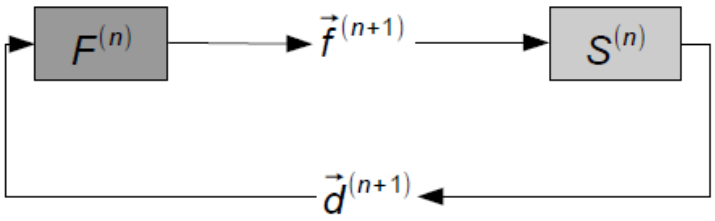

Figure 1: Staggered - Implicit scheme

A key role in time coupling is played by the post-processing technique to be applied at data exchanged between the segregated solvers. A pure implicit coupling without post-processing corresponds to a simple fixed-point iteration, which still has the same stability issues as an explicit coupling. A postprocessing techniques is needed in order to stabilize and accelerate the fixed-point iteration.

In preCICE, three different types of post-processing can be configured: constant (constant under-relaxation), Aitken (adaptive under-relaxation), and various quasi-Newton variants (IQN-ILS also known as Anderson acceleration, IQN-IMVJ or generalized Broyden).

4.2 Load Transfer

In the frame of partitioned approach, the meshes of the different solvers are not conforming at the fluid structure domain interface: they differ in the refinement and gaps and or overlap can also be present. Then a projection of the variables valued with the different solvers at interface should be implemented.

Several authors treat those approaches, showing pro's and con's[21, 22, 23, 24, 25, 26, 27]. There are several criteria which such a data exchange or coupling method ideally should satisfy. The most important are: (i) global conservation of energy over the interface, (ii) global conservation of loads over the interface, (iii) accuracy, (iv) conservation of the accuracy order of the coupled solvers and (v) efficiency, which is defined as a ratio

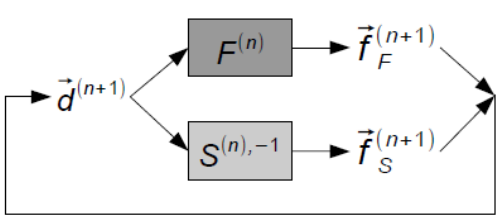

(a) Parallel - Implicit scheme

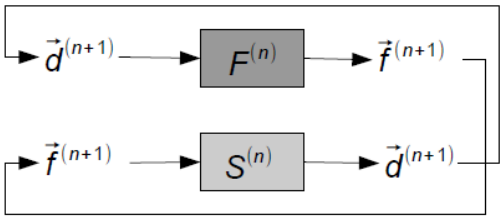

(b) Vectorial system

Figure 2: Flow Chart of Parallel Approaches for fixed point problem solution[8]

between accuracy and computational costs.

According to the main hypotheses on which the transfer operator is built, it is possible to follow a conservative or consistent approach: in the former, the energy is conserved when transferring displacement, pressure and viscous forces over the interface, and it is based on the global conservation of Virtual Work over the interface. In the consistent approach, the constant displacement and constant pressure are exactly interpolated over the interface. In this case the energy conservation is not guaranteed, however can be shown that the error in work transferred can be reduced refining the meshes[23].

A number of methods able to transfer data from grid to grid are available, they are classified in groups: Point-to-Point, Point-to-element and Virtual Surface Method.

In this paper, focus is given on Radial Basis Function (RBF) method, belongs the class of point-to-point schemes, also known as multivariate transfer technique, they are widely adopted in the frame of FSI([28, 29, 30, 31, 24]. Those are mesh-less methods allow to couple structural and fluid domains by reducing them to pure point information. A clear advantage of this technique is the fact that the information about discretization schemes and geometrical typologies are not required.

The value of f at a generic location x, is obtained as a weighted sum of radial basis functions $\phi(|x-x_{C_j}|)$ based on the Euclidean distance between the control points position x_j and x:

$$f(x) = \sum_{j=1}^{N_c} \gamma_j \phi(|x - x_{C_j}|) + q(x) \tag{1}$$

The interpolation condition is also imposed at the control points:

$$f(x_{C_j}) = f_{C_j} \quad for \quad j = 1, \ldots, N_c \tag{2}$$

in order to guarantee the positive definiteness of the RBF problem, the following condition

$$\sum_{j=1}^{N_c} \gamma_j p(x_{C_j}) = 0 \tag{3}$$

should hold for any polynomial p with degree less or equal than the degree of q.

The basis functions investigated in this work, are Thin Plate Spline and Gaussian spline:

- Thin Plate (TPS):
$$\phi(|x|) = |x|^2 \log |x| \tag{4}$$
- Gaussian Spline:
$$\phi(|x|) = \exp^{-a|x|^2} \tag{5}$$

where **a** is a shape parameter.

Radial Basis Functions guarantee a consistent interpolation, but energy is not preserved when loads are transferred over the interface. On the other hand, by adopting a conservative interpolations, the consistency is lost[23]. Moreover, the basis functions need a tuning for the proper setting of the shape parameters.

4.3 CFD ZEN INTERFACE

The CFD ZEN code is coupled with the FEM solver Calculix through the preCICE library. From the FEM side, CalculiX exchanges data with preCICE through a devoted interface[3, 8, 18]. In this section the way the ZEN solver exchanges data with preCICE is described.

The adapter is designed in a less intrusive way, from the point of view of the ZEN solver, since the adapter is totally self-standing and very few coding was made within the solver.

Figure 3 illustrates conceptually how the FSI analysis starts and how data are exchanged during the calculation between the ZEN CFD solver and the ZEN adapter: the latter sends data to preCICE.

The ZEN adapter is coded in cpp language. It is designed to share the CFD variables (i.e. the non-dimensional loads), available after each time step, with the preCICE library.

The simulation starts by launching a shell script that manages the library initialization step. The initialization sets up communications between the adapters to preCICE (from both sides), in order to assign labels, allocate pointers and memory for deforming grids nodes. Moreover, the interface reads information about the face numbering for the exchange of local loads, those have to match the structural mesh.

As the CFD code solves non-dimensional equations, reference dimensions are required in order transform local and global forces, i.e. free-stream static pressure and static temperature, time step and scale length. When launched, the CFD adapter employs the information about free-stream values, to calculate the dimensional loads.

In order to explain how the FSI simulation works, it is convenient to describe first how the CFD solver ZEN performs a flow simulation with dynamic meshes. When a flow simulation with dynamic meshes is running, ZEN requires an updated mesh at each new time step, together with a flag that informs the flow solver whether the time step is completed or the updated mesh has to replace the current one without advancing in time. The latter case happens when implicit coupling occurs and iterative loops are executed with other models. Handling the mesh updating outside the flow solver has several advantages. Among them it allows different models to interact with the configuration geometry (like structural dynamics, body dynamics, configuration changes driven by time laws or any kind of control systems, and so on) and it makes possible to check convergence on both aerodynamic forces and configuration shape by using procedures external to the flow solver. Figure 4 highlights the main tasks performed during a time step. The ZEN flow solver reads a GRID file and writes output files containing (non dimensional) local and global aerodynamic forces, then it waits for an updated GRID. Meanwhile the ZEN

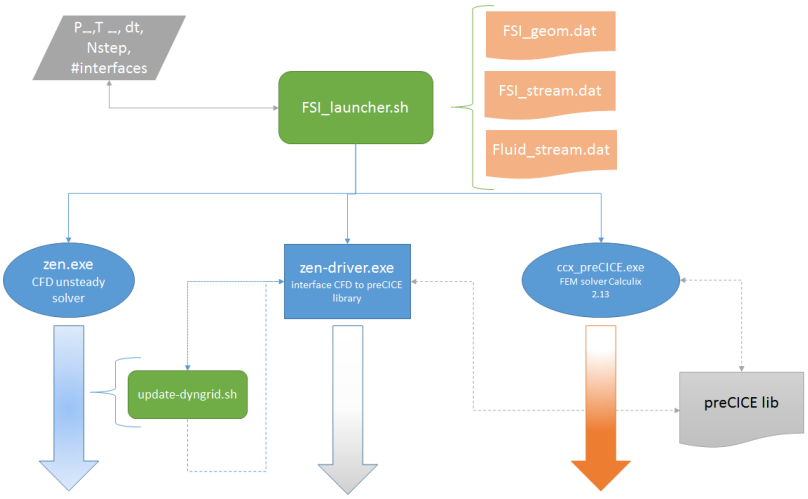

Figure 3: Global chart

adapter reads the aerodynamic forces, computes dimensional loads and sends them to the FEM solver CalculiX through preCICE library. The FEM solver computes displacements, preCICE routines checks loads and displacements for convergence and returns displacements to the adapter, together with information whether to advance in time or to repeat the computation to improve residuals. The adapter writes output files containing the updated shape of configuration surfaces, required to make a new GRID, and the FSI.LOOP flag to inform ZEN about the time step convergence. As the updated surfaces are ready, the procedure to update the dynamic grid produces an updated GRID. The CFD solver checks whether to advance the time step or repeat it by reading the FSI.LOOP flag, then it reads the updated GRID and computes aerodynamic forces again. In figure 4 is also shown how another model which requires aerodynamic forces and computes configuration movements could fit into the procedure, by communicating information to the procedure to update the GRID. More details about the tasks are given in the next paragraph.

5 RESULTS

In this section the output of the 2D panel flutter investigation will be shown, aimed to explore the preCICE capability and to find a better tuning to obtain reliable results in an efficient way. The investigation has regarded the load transfer methods, time-coupling and post-processing scheme, and convergence threshold. Finally, 3D panel flutter results are compared with literature data.

5.1 Numerical Settings

In order to set the numerical methods discussed in previous sections, preCICE can be configured at runtime via an xml file (*precice-config.xml*), where the solvers, the fluid and solid interfaces exchanging data, the kind of data (i.e. scalars, vectors) are defined and

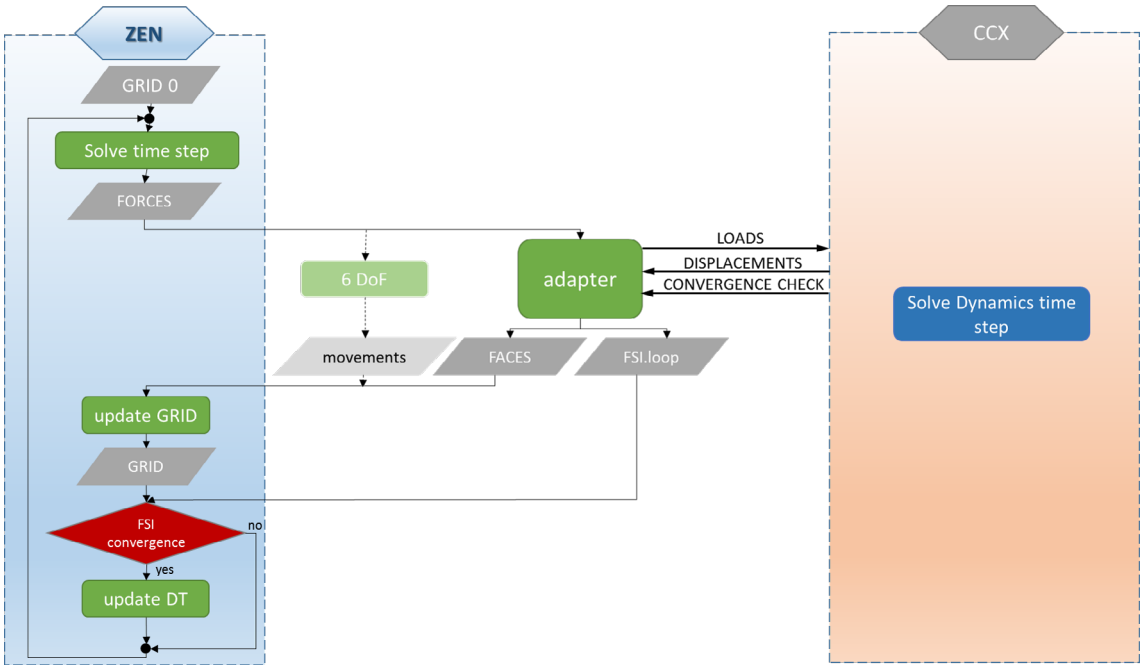

Figure 4: Detailed procedure chart

tagged.

The nature of the problem under investigation requires a strongly coupled approach, as noted also from [11], hence an implicit coupling was chosen. To stabilize and accelerate the fixed-point iteration several post-processing schemes were tested, such as Aitken and the two Quasi Newton variants: IQN-ILS also known as Anderson acceleration, IQN-IMVJ or generalized Broyden.

For implicit coupling scheme, preCICE employs a convergence measure that can be relative or absolute. Here a relative convergence threshold values for displacements and forces is adopted. The FEM solution is taken as reference: all data relative to FEM are post-processed and the convergence is valued on forces and displacement elaborated from the FEM side. The effects of threshold are investigated for forces and displacement ranging from 10^{-3} to 10^{-6} for both displacement and forces.

Other parameters in the coupling schemes and postprocessing have to be set, such as starting relaxation parameters applied to delivered forces and or displacements, maximum number of iterations and extrapolation order. The maximum number of sub-iterations within an implicit coupling loop was set to 30.

On fluid side, in order to compare the results with other authors without the uncertainties stemming from boundary layer thickness and turbulence model effects, the flow is solved with Euler equations.

Even if the non-linear FEM solver allows subcycling within each iteration by changing the time step size to achieve convergence of loads, the current Calculix adapter cannot

manage sub-cycling. Hence the user-defined initial time step is not changed.

5.2 2D Panel Flutter

Here we investigate how the amplitude and the frequency of the LCO changes, according to the critical dynamic pressure, λ, defined as $\lambda^* = \frac{\rho_\infty u_\infty^2 a^3}{D}$, where D is the plate stiffness, $\frac{Eh^3}{12(1-\nu^2)}$. Hence, by changing the Young modulus of the plate, we have obtained a set of λ values at which the analysis are carried out. The mass ratio, μ, calculated as $\mu = \frac{\rho_\infty a}{\rho_m h}$, is kept constant during the simulations and equal to 0.1. The thickness ratio, h/a is equal to 0.002. Free stream Mach number is set to M_∞= 1.2, furthermore pressure and static temperature are fixed and equal to 25000 Pa and 223 K. The panel is pinned at ends, the length is a = 0.5 (m) with uniform thickness $h = 1.00 \times 10^{-3}$ m.

The CFD grid, shown in Figure 5, is made of a single block with three different grid density that will be tested to verify their influence on the LCO calculations showed in the following. The coarser grid, L1, has 105x80 cells, the medium grid L2, 169x80 cells and the finest grid, L3, has 297x80 cells. The flexible interface surface that defines the panel is hence sampled respectively with 64, 128 and 256 cells.

The FEM model of the panel is made of quadratic plane-strain elements with 8 nodes, that would be able to model an infinite panel in the cross-wise direction, in fact, as stated by Calculix[2] manual, they are used to model a slice of a very long structure.

For 2D calculations, the FEM element chosen is a second order Plain - Strain one (CPE8, see in [2]).

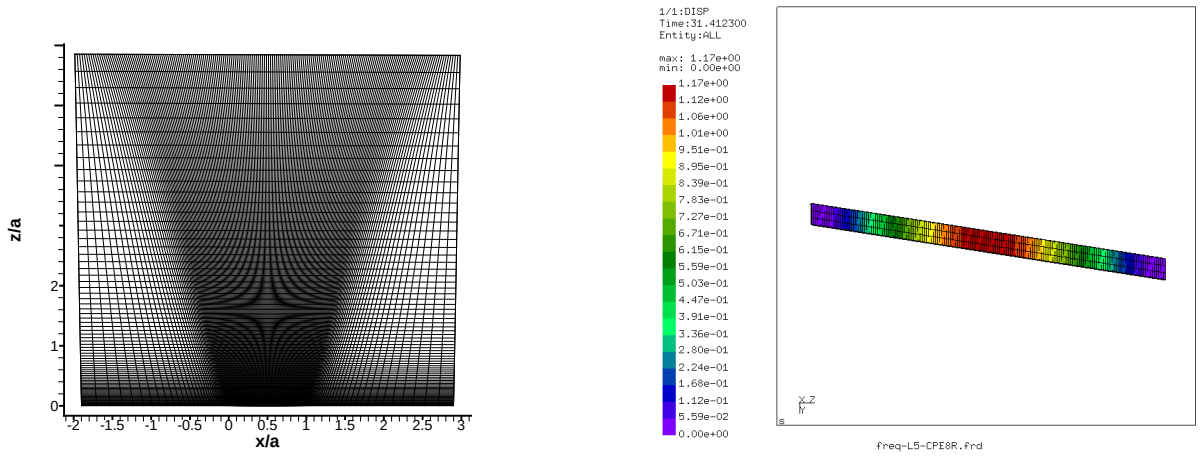

(a) CFD computational domain

(b) FEM panel discretization

Figure 5: CFD grid

Dependency on spatial resolution and time step, from CFD side, is evaluated by considering as a term of comparison the maximum vertical panel displacement, localized at 75% of plate length, normalized with panel thickness, w/h, that identifies the normalized

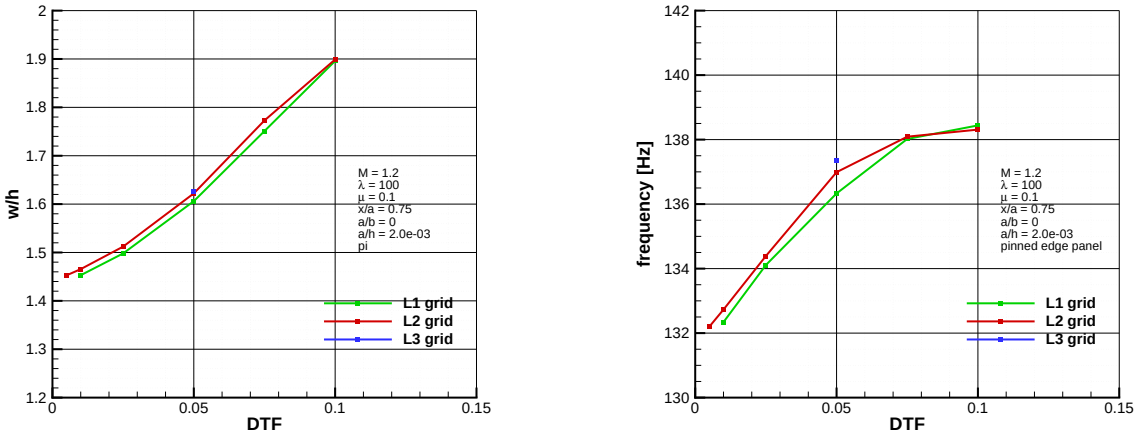

(a) LCO amplitude convergence

(b) LCO frequency convergence

Figure 6: solutions at different time-step size

LCO amplitude. The physical time step of the CFD solver is varied from 0.1 to 0.01 (plus 0.005 for L2 grid), while the grid density changes according to the discretization of the panel, from 64 to 256 CFD grid points.

Figure 6 (a) resume the spatial and temporal study, taking in account both the effects of time and grid refinement and showing the maximum displacement of the point at $0.75a$ versus timestep sampling, for L1, L2 and L3 grid levels: the maximum displacement decreases as timestep is reduced, and slightly increases with grid level refinement.

Figure 6 (b) is referred to the LCO frequencies. The range of frequencies is within 5% with respect to the finest timestep frequency solution on L2 grid level.

In the following, the solution with timestep 0.025 is considered the reference, in order to compare CIRA results with those available in literature.

Figure 7 shows the flowfield pressure coefficient contours in the expansion phase $\phi = 90$, in which are noticeable expansion fans at leading and trailing edges; and compression phase, $\phi = 270$, with presence of shock waves on leading and trailing edges. In this phase the panel showed a deformation in the form of its first natural mode.

In figure 8 are shown both the deformation an the relative pressure coefficient distribution in the expansion and compression stages.

The two solvers start together the integration from free-stream values, and an initial vertical displacement is assigned to the flat panel, equal to $\delta w = w_0 sin^2(\frac{\pi x}{L})$ where w_0, is a constant suitable to produce an initial perturbation. The choice of the modulus of this perturbations influence the time needed to reach the oscillating period of the panel. Even if it can be convenient to simulate the minimum transient time to reach LCO, the modulus of displacements has an influence on the LCO amplitude, as stated by [9]. Figure 9 shows the effects of modulus w_0 on the final LCO.

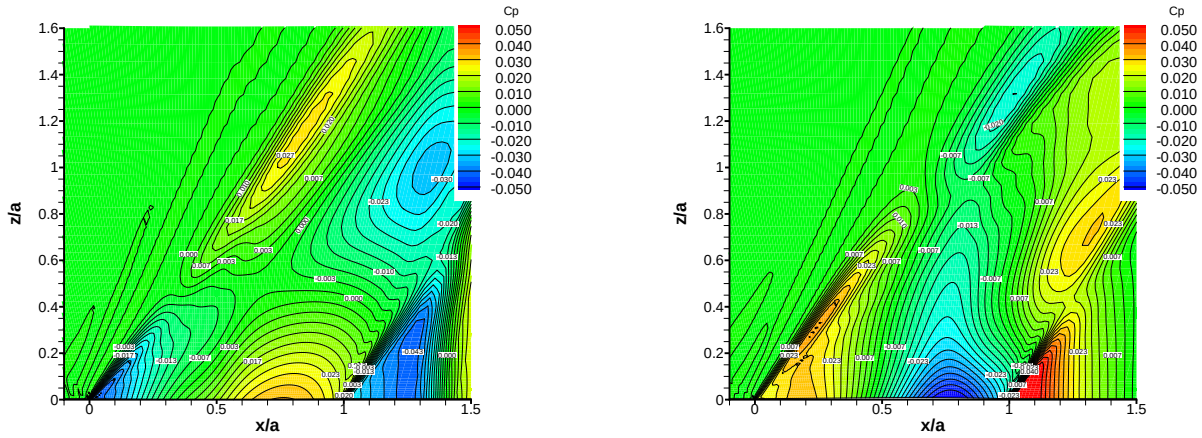

(a) $\phi = 90$, minimum deflection

(b) $\phi = 270$, maximum deflection

Figure 7: Pressure Coefficient contours at minimum and maximum deflection, for dt=0.025

The higher w_0, the shorter time needed to reach a stable LCO. This is not the only effect since the modulus of w/h maximum displacement at 75% of panel length starts to change, up to reach a value of 1.556 with the highest initial perturbation.

Figure 10 shows the time-history, the phase portrait and the spectrum of a point at 75% of panel length, for increasing λ. The LCO becomes wider as the λ grows, but the other noticeable phenomena is that it becomes non-symmetric with larger λ. Such phenomena was evidenced also by Shishaeva[9], even if the analysis was relative to increasing Mach number. The progressive switch from symmetric to non-symmetric LCO is due to the appearance of the second mode, whose frequency yields increase of plate velocity: the flutter is changing from non-resonant to resonant LCO[9]. This is evident the phase-velocity portrait: in the Figure 10 a, it is slightly non-elliptic due to the triple-harmonic, evidenced on the relative frequency spectra on the right. As pressure grows, the 2nd mode amplitude grows as well because to the internal resonance, the velocity increases on phase-velocity portraits, and the relative importance of the 2nd peak of frequency also increases, as it is shown in the spectra on the right.

The results are compared in terms of flutter amplitude and frequency with some data available in literature: figure 16 (a) shows that the maximum displacement foreseen at 0.75a panel point is aligned with recent works that are based on coupling of inviscid CFD codes on fluid side, in the case of pinned panel. Compared to Alder[15], the instabilty of post-flutter is anticipated to lower λ. Figure 16 (b) is relative to LCO frequency: in this case the trend is similar to other data, even if a shift toward higher frequencies can be noted.

After that physical results have been shown, some numerical considerations about the time coupling techniques follow. The average number of coupling iterations, k, shown

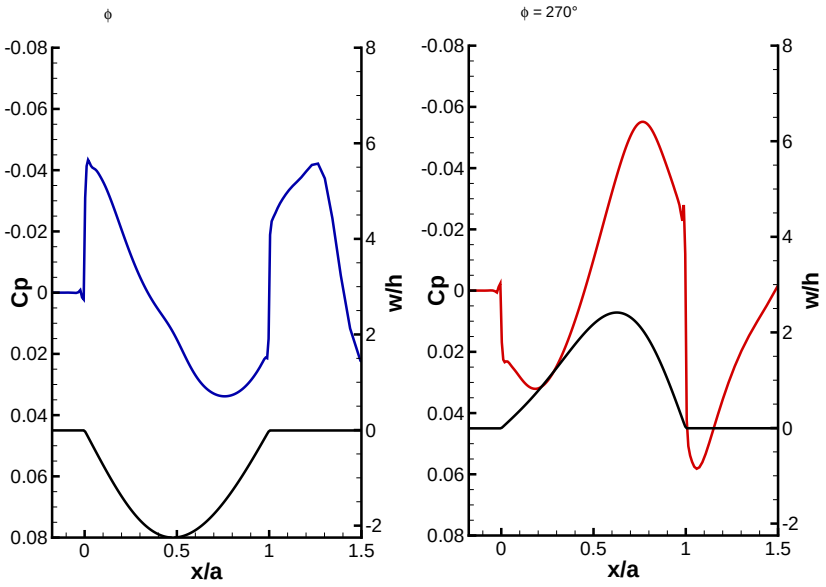

Figure 8: Panel shape and Pressure Coefficient during flutter at M = 1.2, $\lambda = 100$

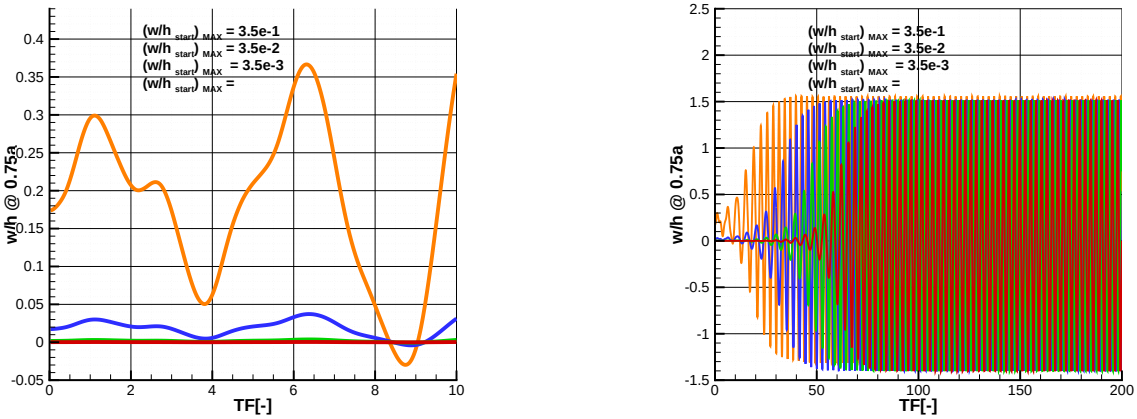

(a) CFD computational domain

(b) FEM panel discretization

Figure 9: Effect of w_0 modulus on panel flutter LCO. DTF = 0.025, level L2 grid

in table 1, are relative to results obtained employing a parallel-implicit coupling with Aitken adaptive relaxation, chosen as post-processing technique, that should stabilize and accelerate the fixed point iteration.

From table 1 can be summarized that, by reducing the timestep, the average amount of sub-iterations decreases, and, when a finer CFD grid is employed, the sub-iterations

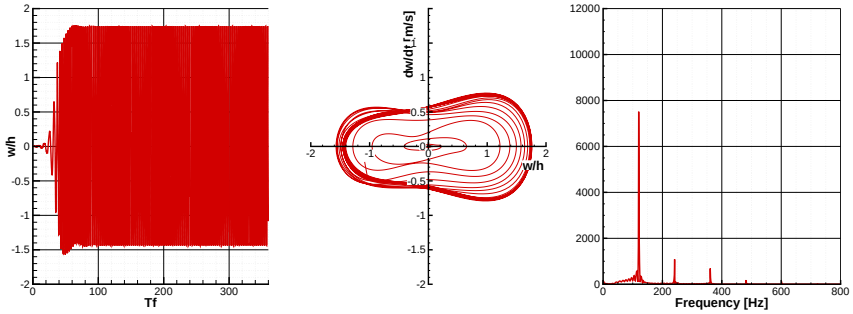

(a) λ=75

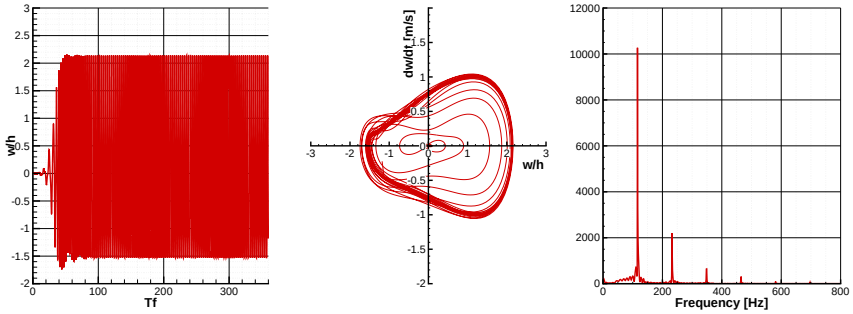

(b) λ=100

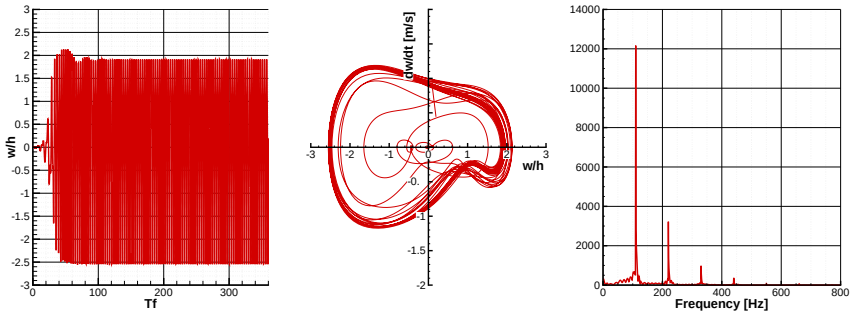

(c) λ=150

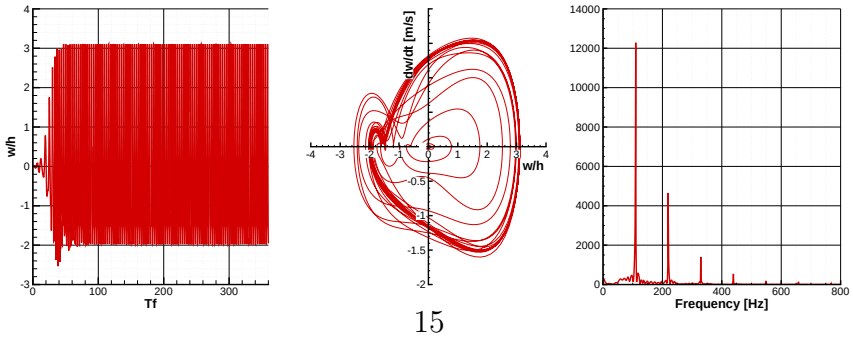

(d) λ=200

Figure 10: LCO, Phase portrait and Spectra of reference point at 0.75a, M=1.2, for different λ, pinned plate.

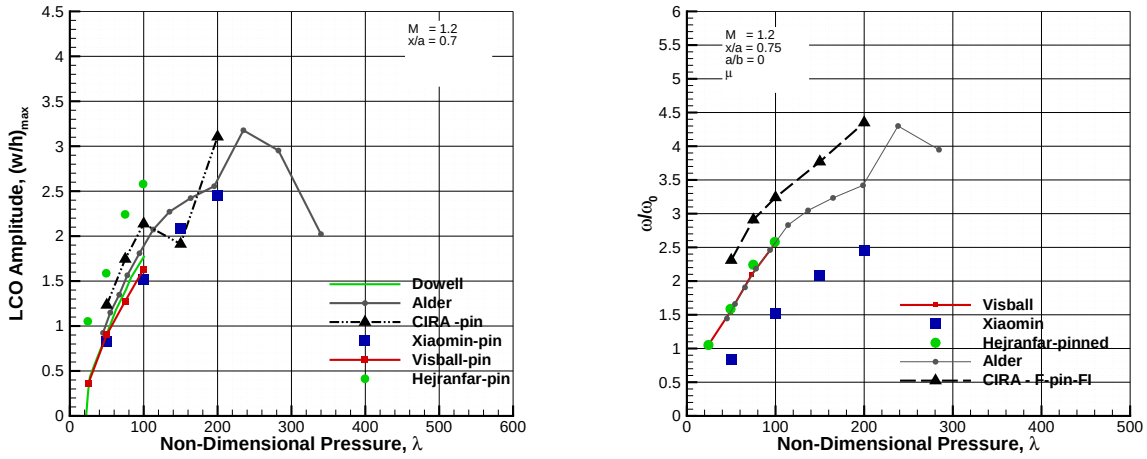

(a) LCO amplitude

(b) LCO frequency

Figure 11: LCO amplitude, pinned panel

needed to reach convergence increases.

The time-coupling methods and post-processing techniques are investigated in the following, in order to verify whether they have an influence on computational costs and/or the quality of the solutions. The post-processing techniques compared are Aitken and the two Quasi Newton variants, IQN-ILS and IQN-IMVJ. Aitken was tested also in the staggered coupling, since it is known from literature that it performs better than in parallel coupling.

Table 2 shows that IQN-ILS performs better of other settings in terms of computational costs.

Not reported in the table is also an analysis carried out with a Staggered explicit coupling, and Aitken post-processing. As expected, this analysis diverges, after 450 timesteps.

Other numerical aspects influence the average number of coupling iterations. First of all, the average number of iterations grows by decreasing the measure of convergence tolerance on the data exchanged by the coupled solvers. When an implicit parallel coupling

DTF/Grid Lev.	L1	L2	L3
0.005	-	4.02	-
0.01	3.97	4.84	-
0.025	4.00	5.25	-
0.05	6.16	6.25	6.57
0.075	7.64	7.74	-
0.1	11.35	11.86	-

Table 1: Average number of coupling iterations for different DTF and Grid Level

is adopted, as in those runs, the relative tolerance of forces and displacement is checked for the convergence within the time-step.

From the table 3 can be noted that, as expected, when the tolerance is small, the iterations needed increases.

Other parameter that depends on the post-processing coupling and that can influence the results, is the initial value of the relaxation factor (common to Aitken and Quasi Newton methods): a larger value of ω (0.1) has produced a longer convergence history than smaller values (i.e. $\omega = 0.01$).

In the two Quasi Newton variants, a relevant factor is the timestep-reused parameter, that limits the previous iterations used to generate the data basis for Jacobian estimation. To set this, some preliminary evaluations were needed.

5.3 3D Panel Flutter

The 3D panel test constitutes a more significant test case for the validation of the FSI environment.

The FEM model of a square panel, $a/b = 1$, is a 20x20x2 solid elements (*C3D20R*). The CFD grid has 64x64 cells on panel, and 112x112x80 in stream-wise, span-wise and normal direction respectively. Furthermore, a rectangular plate $a/b = 0.5$ is also analysed at the same conditions. The square plate results are relative to clamped and pinned boundary conditions (all four edge), while the rectangular plate is clamped at all four edges.

The free-stream flow conditions and the structural plate properties are the same as the 2D simulations: Mach 1.2 and *lambda*=250,300 and 350.

Figure 12 (a) and (b) show the surface pressure contours for square and rectangular plate, respectively, at maximum upward deflection. Both are symmetric with respect to the centerline at $y/b = 0$.

A sequence of compression, expansion and finally a shock wave can be noted in both cases, with larger gradient in the $a/b = 0.5$ case.

Figure 13 (a) and (b) show, for square and rectangular plate respectively, the normalized displacements, w/h, on the panel at $\lambda = 300$, when it is at the maximum upward deflection. The results are symmetric with respect to the centerline. The peak of the deflection is found at about $x/a = 0.66$: those results are comparable to the ones shown in [11] for the case of the squared plate.

Coupling	**k**
Stag-Impl Aitken	4.05
Par-Impl Aitken	6.25
Par-Impl IQN-ILS	3.27
Par-Impl IQN-IMVJ	4.83

Table 2: Average number of coupling iterations per coupling type (DTF=0.05, L2 grid; point at x=0.75a.)

ϵ_{forces};$\epsilon_{displacements}$	**k**
1e-3;1e-3	2.94
1e-4;1e-4	4.60
1e-5;1e-3	3.27
1e-5;1e-5	7.16
1e-6;1e-6	15.76

Table 3: Average number of coupling iterations: tolerance effects (DTF=0.05, L2 grid; point at x=0.75a.)

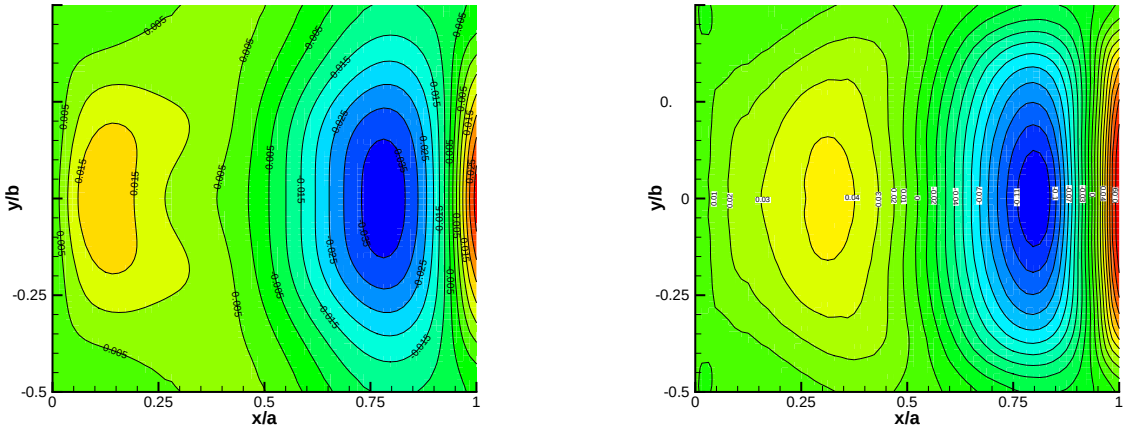

(a) $a/b = 1$ (b) $a/b = 0.5$

Figure 12: Surface pressure contours for $(M = 1.2, \lambda = 300)$ at maximum upward deflection

Figure 14 and 15 show the time history, phase portrait and frequency for the 3D panel at $\lambda = 300$, with $a/b = 1$ and $a/b = 0.5$, respectively. The reference point considered is the same of previous figures at 0.75 of x/a: the three dimensional effects are evident in phase portraits: when $a/b = 0.5$ the portrait is quite similar to the 2D results shows in fig. 10.

Figures 16 (a) and (b) show the LCO amplitude and frequency versus dynamic pressure of a point at $y = 0.5b$ and $x = 0.75a$ of the square plate, with clamped and pinned edges. The calculations here performed show good agreement with literature, especially at high pressure levels. The fundamental linear frequency for a 3D panel is valued by $\omega_0 = \pi^2(1 + AR^2)\sqrt{\frac{D}{\rho_s h a^4}}$[11], where $AR = \frac{a}{b}$.

Finally, some considerations from the numerical point of view. In the 3D simulations, the Par-Impl IQN-ILS time coupling is chosen. The average number of coupling iterations for the square plate is $k = 3.1$, while for the rectangular plate $k = 2.9$. A difference between the two cases is the average amount of iterations that the CFD solver has to run in order to reach convergence in the time step: it is lower for the case with $a/b = 1.0$ (72)

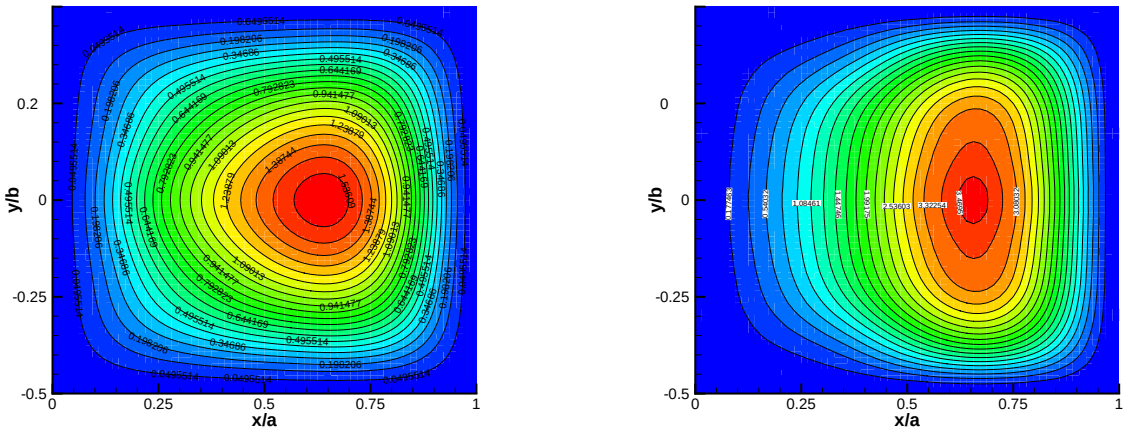

(a) $a/b = 1$ (b) $a/b = 0.5$

Figure 13: Surface deflection contours for $(M = 1.2, \lambda = 300)$ at maximum upward deflection

than for the case $a/b = 0.5$ (99).

6 CONCLUSIONS

This report has described the development and validation of a new framework able to face with FSI problems. Partitioned approach is followed to take advantage of already existing codes: in house CFD solver, and open source FEM. An adapeter was developed, by using the preCICE library, that 'glues' the CFD code with FEM solver, Calculix. Classical FSI problem of 2D and 3D panel flutter at supersonic speed have been simulated with strongly-coupled partitioned approach and the results are compared with available literature showing good agreement.

REFERENCES

[1] Marongiu C, Catalano P, A. M. e. a., "U-ZEN: a computational tool solving U-RANS equations for industrial unsteady applications," *34th AIAA fluid dynamics conference, Portland OR*, No. AIAA Paper 2004-2345, 2004.

[2] Dhondt, G., *CalculiX CrunchiX USER'S MANUAL version 2.13*, 08 2017.

[3] Bungartz, H.-J., Lindner, F., Gatzhammer, B., Mehl, M., Scheufele, K., Shukaev, A., and Uekermann, B., "preCICE – A Fully Parallel Library for Multi-Physics Surface Coupling," *Computers and Fluids*, Vol. 141, 2016, pp. 250—-258.

[4] Vitagliano, P. L., Minervino, M., Quagliarella, D., and Catalano, P., "A conservative sliding mesh coupling procedure for U-RANS flow simulations," *Aircraft Engineering and Aerospace Technology*, Vol. 88, No. 1, 2016, pp. 151–158.

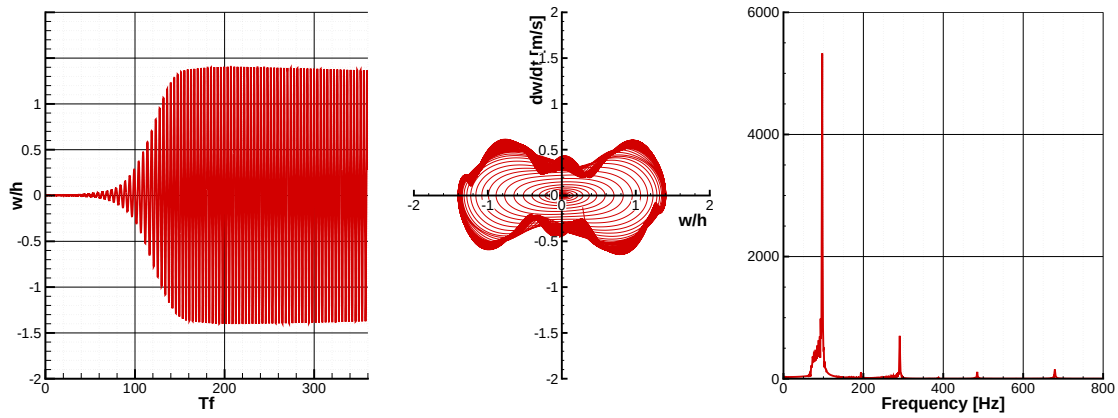

Figure 14: LCO, phase portrait and spectra of point at 0.75a,0.5b, $\lambda = 300$, $a/b = 1$, clamped edges

[5] Farhat, C. and Geuzaine, P., "Design and analysis of robust ALE time-integrators for the solution of unsteady flow problems on moving grids," *Computer Methods in Applied Mechanics and Engineering*, Vol. 193, No. 39, 2004, pp. 4073 – 4095, The Arbitrary Lagrangian-Eulerian Formulation.

[6] Farhat, C., Lesoinne, M., and LeTallec, P., "A conservative algorithm for exchanging aerodynamic and elastodynamic data in aeroelastic systems," *Aerospace Sciences Meetings*, American Institute of Aeronautics and Astronautics, Jan. 1998, pp. –.

[7] Dhondt, G., *The Finite Element Method for Three-Dimensional Thermomechanical Applications*, Wiley, 2004.

[8] Uekermann, B., *Partitioned Fluid-Structure Interaction on Massively Parallel Systems*, Dissertation, Institut für Informatik, Technische Universität München, Oct. 2016.

[9] Shishaeva, A., Vedeneev, V., and Aksenov, A., "Nonlinear single-mode and multi-mode panel flutter oscillations at low supersonic speeds," *Journal of Fluids and Structures*, Vol. 56, 2015, pp. 205 – 223.

[10] DAVIS, G. and BENDIKSEN, O., "Transonic panel flutter," *Structures, Structural Dynamics, and Materials and Co-located Conferences*, American Institute of Aeronautics and Astronautics, April 1993, pp. –.

[11] GORDNIER, R. and VISBAL, M., "DEVELOPMENT OF A THREE-DIMENSIONAL VISCOUS AEROELASTIC SOLVER FOR NONLINEAR PANEL FLUTTER," *Journal of Fluids and Structures*, Vol. 16, No. 4, 2002, pp. 497 – 527.

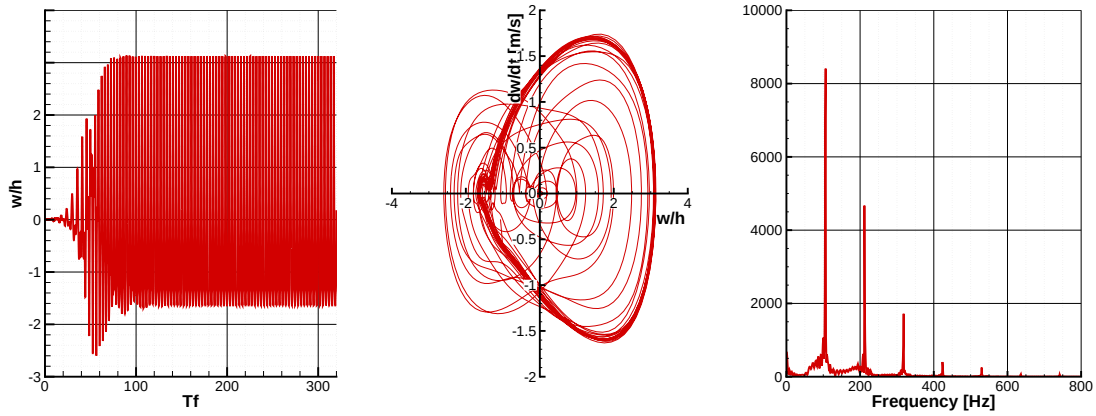

Figure 15: LCO, phase portrait and spectra of point at 0.75a,0.5b, $\lambda = 300$, $a/b = 0.5$, clamped edges

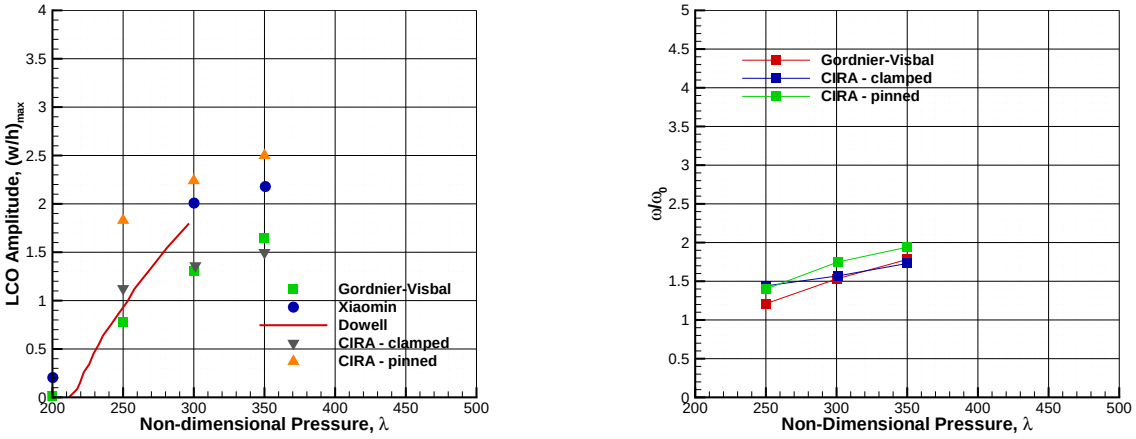

(a) Limit-cycle amplitude

(b) Limit-cycle frequency

Figure 16: Limit-cycle versus dynamic pressure for 3D panel flutter, $M = 1.2$

[12] Hashimoto, A., Aoyama, T., and Nakamura, Y., "Effects of Turbulent Boundary Layer on Panel Flutter," *AIAA Journal*, Vol. 47, No. 12, Dec. 2009, pp. 2785–2791.

[13] Anjyo, K., Lewis, J. P., and Pighin, F., "Scattered data interpolation for computer graphics," *ACM SIGGRAPH 2014 Courses*, ACM, 2014, p. 27.

[14] DOWELL, E. H., "Generalized aerodynamic forces on a flexible plate undergoing transient motion in a shear flow with an application to panel flutter," *AIAA Journal*, Vol. 9, No. 5, May 1971, pp. 834–841.

[15] Alder, M., "Development and Validation of a Partitioned Fluid-Structure Solver for Transonic Panel Flutter with Focus on Boundary Layer Effects," *AIAA AVIATION Forum*, American Institute of Aeronautics and Astronautics, June 2014, pp. –.

[16] Hejranfar, K. and Azampour, M., "Simulation of 2D fluid-structure interaction in inviscid compressible flows using a cell-vertex central difference finite volume method," *Journal of Fluids and Structures*, Vol. 67, 2016, pp. 190 – 218.

[17] Catalano, P. and Amato, M., "An Evaluation of RANS Turbulence Modeling for Aerodinamic Applications," *Aerospace Science and Technology*, Vol. 7, No. 7, 2003, pp. 493–590.

[18] Rusch, A., *Extending SU2 to fluid-structure interaction via preCICE.*, Master's thesis, Munich School of Engineering, Technical University of Munich, 2016.

[19] Romanelli, G., Castellani, M., Mantegazza, P., and Ricci, S., "Coupled CSD/CFD non-linear aeroelastic trim of free-flying flexible aircraft," *Structures, Structural Dynamics, and Materials and Co-located Conferences*, American Institute of Aeronautics and Astronautics, April 2012, pp. –.

[20] Kassiotis, C., *Nonlinear Fluid-Structure Interaction: a Partitioned Approach and its Application Through Component Technology*, Theses, Université Paris-Est, Nov. 2009.

[21] Jiao, X. and Heath, M. T., "Common-refinement-based data transfer between non-matching meshes in multiphysics simulations," *International Journal for Numerical Methods in Engineering*, Vol. 61, No. 14, 2004, pp. 2402–2427.

[22] Ross, M. R., Sprague, M. A., Felippa, C. A., and Park, K., "Treatment of acoustic fluid–structure interaction by localized Lagrange multipliers and comparison to alternative interface-coupling methods," *Computer Methods in Applied Mechanics and Engineering*, Vol. 198, No. 9, 2009, pp. 986–1005.

[23] Bogaers, A. E. J., *Efficient and robust partitioned solution schemes for fluid-structure interactions*, Theses, Faculty of Engineering and the built environment - Univeristy of Cape Town, January 2015.

[24] Quaranta, G., Masarati, P., and Mantegazza, P., "A conservative mesh-free approach for fluid-structure interface problems," *International Conference for Coupled Problems in Science and Engineering, Greece*, 2005.

[25] Jaiman, R., Jiao, X., Geubelle, P., and Loth, E., "Assessment of conservative load transfer for fluid–solid interface with non-matching meshes," *International Journal for Numerical Methods in Engineering*, Vol. 64, No. 15, 2005, pp. 2014–2038.

[26] Cebral, J. R. and Lohner, R., "Conservative Load Projection and Tracking for Fluid-Structure Problems," *AIAA Journal*, Vol. 35, No. 4, April 1997, pp. 687–692.

[27] Jaiman, R., Geubelle, P., Loth, E., and Jiao, X., "Transient fluid-structure interaction with non-matching spatial and temporal discretizations," *Computers and Fluids*, Vol. 50, No. 1, 11 2011, pp. 120–135.

[28] Harder, R. L. and Desmarais, R. N., "Interpolation using surface splines." *Journal of aircraft*, Vol. 9, No. 2, 1972, pp. 189–191.

[29] APPA, K., "Finite-surface spline," *Journal of Aircraft*, Vol. 26, No. 5, May 1989, pp. 495–496.

[30] Ahrem, R., Beckert, A., and Wendland, H., "A new multivariate interpolation method for large-scale spatial coupling problems in aeroelasticity," 2005.

[31] Rendall, T. C. S. and Allen, C. B., "Improved radial basis function fluids-structure coupling via efficient localized implementation," *International Journal for Numerical Methods in Engineering*, Vol. 78, No. 10, 2009, pp. 1188–1208.